ARTICLE

Check for updates

Feasibility of gasifying mixed plastic waste for hydrogen production and carbon capture and storage

Kai Lan[1] & Yuan Yao [1✉]

Waste plastic gasification for hydrogen production combined with carbon capture and storage is one technology option to address the plastic waste challenge. Here, we conducted a techno-economic analysis and life cycle assessment to assess this option. The minimum hydrogen selling price of a 2000 oven-dry metric ton/day mixed plastic waste plant with carbon capture and storage is US$2.26–2.94 kg^{-1} hydrogen, which can compete with fossil fuel hydrogen with carbon capture and storage (US$1.21–2.62 kg^{-1} hydrogen) and current electrolysis hydrogen (US$3.20–7.70 kg^{-1} hydrogen). An improvement analysis outlines the roadmap for reducing the average minimum hydrogen selling price from US$2.60 to US$1.46 kg^{-1} hydrogen, which can be further lowered to US$1.06 kg^{-1} hydrogen if carbon credits are close to the carbon capture and storage costs along with low feedstock cost. The life cycle assessment results show that hydrogen derived from mixed plastic waste has lower environmental impacts than single-stream plastics.

[1] Center for Industrial Ecology, Yale School of the Environment, Yale University, 380 Edwards Street, New Haven, CT 06511, USA. ✉email: y.yao@yale.edu

Plastic is a crucial material in many sectors, including construction, packaging, transportation, electronics, textiles, and others[1,2]. The last half century has witnessed the rapidly increasing demand and production of plastics[1], resulting in considerable plastic waste due to the low plastic recycling rate. From 1950 to 2015, only 9% of the cumulative plastic waste generation (6300 million metric tons (Mt)) was recycled, compared to over 60% discarded (accumulating in landfills or in the natural environment)[1]. The landfilled or disposed plastic wastes and their fragments, i.e., microplastics and nanoplastics, have caused increasing environmental concerns[3–6]. Increasing plastic recycling is one essential strategy to reduce plastic waste disposal[7]. There are two common types of plastic recycling, mechanical (e.g., magnetic density separation) and chemical recycling (e.g., gasification)[7]. Recently, another type of recycling method, solvent-based recycling (or referred as physical recycling), is also attracting attention[8]. The challenges of plastic mechanical recycling include thermal-mechanical degradation (e.g., caused by heating and mechanical shearing of polymer)[7], plastic degradation (e.g., caused by photo-oxidation process during lifetime), incompatibility among different polymers when recycling blended plastics[9], and contaminations (e.g., coating, ink, additives, metal residues or cross-contaminations among different plastic streams)[9,10]. Some waste plastics are hard to be mechanically recycled due to low bulk density (e.g., films), lightweight (e.g., polystyrene (PS)), low economic value (e.g., PS), and carbon-black pigments that absorb infrared light and confound the sorting machine[9,11]. Hence, relying on the traditional mechanical recycling method alone is insufficient to address the increasing volume and variety of plastic waste. Compared to mechanical recycling, thermochemical methods, as one type of chemical recycling, have advantages in processing plastic wastes that are difficult to be depolymerized, or mechanically recycled due to economic or technical barriers[7,12]. Thermochemical processes include pyrolysis and gasification, which have potentials to treat waste plastics with high energy, carbon, and hydrogen content, and low moisture content[13]. Thermochemical processes can produce a variety of products, and hydrogen is one product with a mature and growing market[14]. Hydrogen is an important industrial gas widely used in the oil refining and chemical industries, it can also be used as a clean energy source for transportation[15]. U.S. Department of Energy (DOE) estimated the U.S. hydrogen demand as high as 22–41 Mt per year by 2050, given the enormous need for clean energy[16]. Currently, 96% of hydrogen production uses fossil fuel reforming (e.g., petroleum, natural gas, and coal)[15]. Converting MPW to hydrogen has the potential to reduce fossil fuel demand for hydrogen production and address worldwide challenges of rapidly growing plastic wastes[17]. For example, the U.S. DOE Hydrogen Program Plan highlighted "diverse domestic resources" including waste plastics as an important source of hydrogen production[16].

Since most plastics are made from fossil fuels, it is necessary to mitigate the fossil-based carbon emissions during the thermochemical conversion of MPW to hydrogen[1,15]. Carbon capture and storage (CCS) is an important technology to mitigate climate change by capturing and geologically storing CO_2 (ref. [18]). Coupling hydrogen production with CCS offers a means to produce low-carbon hydrogen[1,15]. For the large-scale development and implementation of plastic recycling technologies, it is critical to understand the economic feasibility and environmental performance of plastic waste to hydrogen pathway with/without CCS and policy incentives, as well as to identify the key drivers and future improvement opportunities.

Techno-economic analysis (TEA) is one of the most widely used tools to assess the economic and technical feasibility of emerging technologies[19–24]; Life Cycle Assessment (LCA) is a standardized tool to quantify life-cycle environmental impacts[25–31]. Several studies have used TEA to evaluate the economic feasibility or LCA to assess the environmental implications of plastic wastes to energy products (see Supplementary Note 1 for literature review). However, few studies have explored the economic and environmental implications of MPW to hydrogen at a large scale with CCS, or investigated the drivers of the economic and environmental performance of MPW compared to single-stream recycled plastic.

To fill the knowledge gap, we conducted a TEA and LCA to evaluate the economic and environmental performance of hydrogen production from MPW and single-stream recycled plastic in the U.S. and identify cost reduction opportunities. A mechanistic process simulation model (see Fig. 1 for system boundary and plant process flow diagram, and see Methods for details) was developed in Aspen Plus[32] to provide rigorous
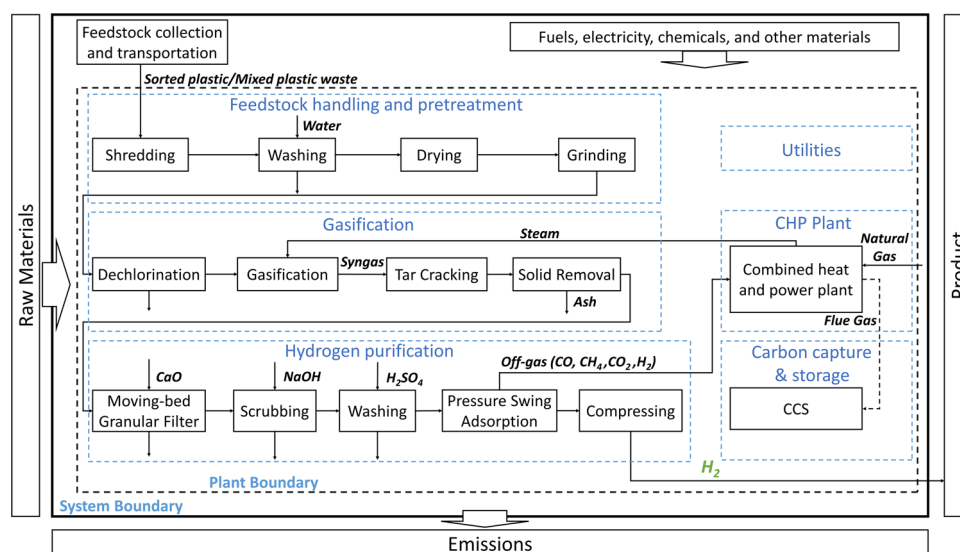
Fig. 1 System boundary of Life Cycle Assessment and flow diagram of the plant. The flow diagram inside the plant boundary includes five main areas, including feedstock handling and pretreatment, gasification, hydrogen purification, combined heat and power (CHP) plant, and utilities, along with carbon capture and storage (CCS) for scenario analysis.
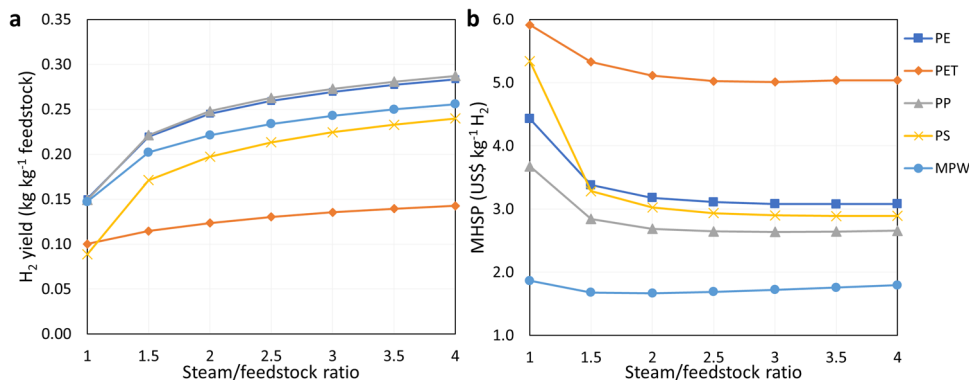
Fig. 2 Hydrogen yield and minimum hydrogen selling price of varied steam/feedstock ratio in Scenario 1 at 2000 oven-dry metric tons per day.
a Hydrogen yield. **b** minimum hydrogen selling price.

engineering estimation of mass and energy balance data used in TEA and LCA. The minimum hydrogen selling price (MHSP) was selected to assess the economic feasibility of the hydrogen plant[33]. For life-cycle environmental impact assessment (LCIA), TRACI 2.1 by U.S. Environmental Protection Agency (EPA) and Global Warming Potential (GWP) factors (100-year time horizon) by the Intergovernmental Panel on Climate Change (IPCC) 2021 (in the sixth assessment) are used[34,35]. Different scenarios were designed to examine the impacts of varied feedstock compositions, plant capacities, CCS adoption, and policy incentives. A sensitivity analysis was conducted to identify key drivers of production costs. Finally, an improvement analysis outlined the roadmap for reducing production costs by improving key technical and economic parameters. This study contributes to the fundamental understanding of the economic and environmental performance of MPW to hydrogen pathway, which will inform the waste management industry with economically and environmentally preferable system design and shed light on opportunities to reduce cost and environmental burden.

Results

In this study, the scenario analysis was used to evaluate the impacts of feedstock types, plant capacities, CCS adoption, and carbon credits, as shown in Supplementary Table 1. Scenario 1 depicts the baseline cases without CCS; Scenario 2 describes the cases with CCS but no carbon credit available; Scenario 3 considers CCS and carbon credits for capturing and storing CO_2. In each scenario, five different feedstock cases are included, namely one MPW case and four single-stream feedstock cases (polyethylene (PE), polyethylene terephthalate (PET), polypropylene (PP), and PS) (see Methods). Many studies have explored the thermochemical conversion of single-stream or mixed plastics, but few studies have compared the economic and environmental performance of hydrogen derived from gasifying the single-stream plastics and MPW[13,17,36–43]. For each feedstock case, the varied steam/feedstock ratios were studied to reach the optimal MHSP. Five plant capacities (100–2000 oven-dry metric ton (ODMT) per day of plastic fed in) are compared to explore the impacts of capacities on the MHSP. The capacities were selected based on the current estimation of plastic wastes landfilled in the U.S. The quantity of state-level landfilled plastic waste in 2019 exceeds 250,000 t year^{-1} (762 t day^{-1}) in 35 states and exceeds 1000,000 t year^{-1} (3049 t day^{-1}) in 12 states[44].

Effects of varied steam/feedstock ratio on MHSP. As the gasification utilizes steam as a gasifying agent, the steam/feedstock ratio (S/F ratio in kg steam to oven dry kg feedstock) directly influence the hydrogen yield and further impact the MHSP (see

Methods). To locate the optimal S/F ratio for each case, this study varies the S/F from 1.0 to 4.0 to derive varied H_2 yield (Fig. 2a) and baseline MHSP (Scenario 1 without CCS) (Fig. 2b) (see Methods Section Process simulation model of the hydrogen plant for more information on feedstock composition and TEA details). For five feedstock cases, our findings suggest the optimal (lowest) MHSP is US$3.08 kg^{-1} at S/F 3.5 for PE, US$5.01 kg^{-1} at S/F 3.0 for PET, US$2.64 kg^{-1} at S/F 3.0 for PP, US$2.89 kg^{-1} at S/F 3.5 for PS, and US$1.67 kg^{-1} at S/F 2.0 for MPW (Fig. 2). Among different plastic in Fig. 2a, PP and PE have the highest H_2 yields (0.15–0.29 kg H_2 per kg feedstock), and the results of the two cases almost overlap. PET shows the lowest H_2 yield (0.10–0.14 kg H_2 per kg feedstock) due to the low carbon content (62.5%), hydrogen content (4.2%), and Lower Heating Value (LHV, 22.1 MJ kg^{-1})[45] (see Supplementary Table 2). In Fig. 2a, the rising S/F ratio increases the H_2 yield, which is aligned with the previous literature[40]. However, the higher H_2 yield does not necessarily lead to lower MHSP in Fig. 2b.

In Fig. 2b, the MHSP without CCS (Scenario 1) of all feedstock cases decrease first and then increases. This non-linear phenomenon is caused by the different impacts of the S/F ratio on H_2 yields and energy costs. The higher S/F ratio raises energy demand for steam production and reduces electricity generation in the CHP plant, resulting in higher energy costs. The higher S/F ratio also leads to a larger flow volume in equipment and further increases the capital cost. On the contrary, increased H_2 yield enabled by the higher S/F ratio decreases production costs, resulting in the initial reduction of MHSP (see Supplementary Fig. 1). As the S/F ratio further increases, energy costs increase substantially and overweigh the reduction enabled by increased H_2 yield, resulting in the overall growth of MHSP. For example, in the MPW case in Fig. 2b, from the S/F ratio 1.0 to 1.5, MHSP decreases from US$1.86 kg^{-1} H_2 to US$1.68 kg^{-1} H_2, and further lowers to US$1.67 kg^{-1} H_2 with 2.0 S/F ratio, which is the lowest MHSP point. Crossing over S/F ratio 2.0, MHSP increases to US$1.79 kg^{-1} at 4.0 S/F ratio. This result shows the mixed impacts of the S/F ratio and plastic waste type on MHSP; it also highlights the importance of choosing the optimal S/F ratio by conducting an integrated process simulation and TEA for simultaneous consideration of technical and economic performance.

Effects of varied feedstock costs on MHSP. Another factor affecting the economic feasibility is feedstock cost. Supplementary Fig. 2 displays an example of how the MHSP in Scenario 1-MPW (2000 ODMT per day) changes when the feedstock cost of MPW varies (US$75.5 ODMT^{-1} was used for results shown in Fig. 2). The substantial variations of MPW feedstock cost are caused by the differences in availability, transportation distances, or selling
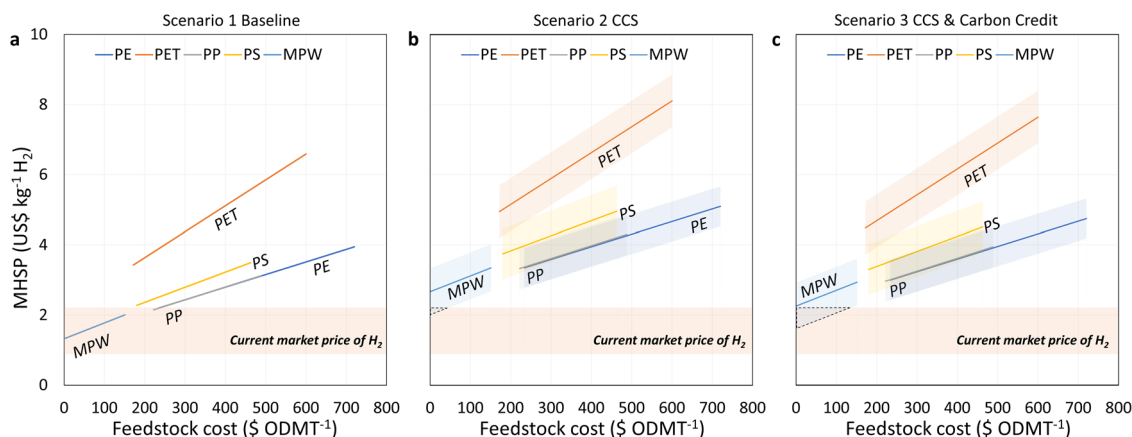
Fig. 3 Minimum hydrogen selling price of 2000 oven dry metric tons per day hydrogen plants in Scenarios 1–3 with varied feedstock cost. a Scenario 1 baseline; **b** Scenario 2 CCS; **c** Scenario 3 CCS & Carbon Credit. The shaded areas of Scenario 2 (Fig. 3b) and Scenario 3 (Fig. 3c) cover the uncertainty of MHSP results with varied CCS costs. The triangular dashed line boxes in Fig. 3b and c mark the areas where MHSP is economically competitive compared with the current market price of H_2. The current market price of fossil-based hydrogen ranges from US\$0.91 to US\$2.21 kg^{-1} H_2 (without CCS) (see Supplementary Table 3), which are highlighted as economic benchmarks.

prices set by material recovery facilities (MRF)[46]. Based on Supplementary Fig. 2, when the feedstock cost of MPW varies, the S/F ratio will need to be adjusted accordingly to reach the optimal MHSP. For example, the optimal S/F ratio is 2.0 at US\$75.5 ODMT^{-1}, and rises to 3.0 at US\$300 ODMT^{-1}. This phenomenon is caused by the increasingly dominated role of feedstock cost as it increases. The higher the feedstock cost is, the higher contribution it makes to the total MHSP, resulting in the higher optimal S/F ratio (as the higher S/F ratio leads to lower feedstock cost per kg of H_2, see Supplementary Fig. 3). A similar trend is observed for the single-stream plastics (see Supplementary Figs. 4–7). This result highlights the operational-level necessity of adjusting the S/F ratio according to the varied feedstock cost of plastic wastes.

**Economic competitiveness of plastic waste derived hydrogen**. Figure 3 shows the MHSP of hydrogen plants at 2000 ODMT per day of plastic waste in three scenarios (see Supplementary Fig. 8 for the MHSP of varied capacities). The detailed results of capital investment and operating cost are available in Supplementary Notes 2 and 3, Supplementary Figs. 9–11. In Fig. 3, the feedstock cost range was collected from the literature (see Supplementary Note 4). Waste plastic-derived hydrogen is economically competitive when the MHSP is within the range of the current market price of hydrogen.

Without CCS, only the MPW case shows competitive MHSP (US\$1.33–\$2.00 kg^{-1} H_2 for feedstock cost \$0–\$151 ODMT^{-1}), compared with current fossil-based hydrogen, as shown in Fig. 3a. The economic competitiveness of other cases depends on the feedstock costs (except for PET and PS whose MHSP is always higher than the fossil-based H_2). For example, PE needs a feedstock cost under US\$236 ODMT^{-1} to be economically competitive; PP needs a feedstock cost under US\$238 ODMT^{-1}. These thresholds are towards the lower bounds of feedstock costs of PE, and PP, indicating the limited possibility of utilizing recycled single plastic streams for hydrogen production in most cases, given the high feedstock costs caused by expensive sorting and processing in MRF. Some strategies have been proposed in the literature to overcome the cost barriers, e.g., advocating for "design for recycling" to lower the recycling cost[47], improving waste collection and separation infrastructures[11], optimizing municipal waste collection systems prior to MRF[48], and adopting cost-effective technologies (e.g., triboelectrostatic separation) in MRF[49].

When CCS cost (see Supplementary Notes 4 and 5) is added in Fig. 3b, only Scenario 2-MWP achieves MHSP comparable to fossil-based H_2 (as marked with the triangular dashed line box) when the CCS cost and the MPW feedstock cost is low. For example, in Scenario 2-MPW, lowering the MHSP to US\$2.21 kg^{-1} H_2 (the highest price of H_2 from fossil fuels without CCS) requires the CCS cost to be lower than US\$53 t^{-1} CO_2 at US\$46 ODMT^{-1} MPW, or lower than US\$69 t^{-1} CO_2 at US\$0 ODMT^{-1} MPW. These expected low CCS costs are at the lower bounds of current CCS costs ranging from US\$53–\$157 t^{-1} CO_2. With policy supports such as carbon credits in Fig. 3c (discussion in next paragraph), the MPW case can be more economically favorable (triangular dashed line box in Fig. 3c). In addition, the cost increases caused by CCS adoption are different across fives cases. Specifically, from Scenario 1 to Scenario 2, MHSP increased by US\$0.58–\$1.71 kg^{-1} H_2 for PE, US\$0.76–\$2.26 kg^{-1} H_2 for PET, US\$0.53–\$1.76 kg^{-1} H_2 for PP, US\$0.74–\$2.18 kg^{-1} H_2 for PS, and US\$0.68–\$2.00 kg^{-1} H_2 for MPW. Such differences are mainly caused by feedstock properties (i.e., compositions and LHV), H_2 yield, and natural gas consumption of different plastics. These results highlight the need to consider the differences among plastic feedstocks and economic implications when incorporating CCS into plastic recycling.

With the incentive credit in Fig. 3c, the MHSP of MPW can be reduced by US\$0.41 kg^{-1} H_2. Hence, in Scenario 3, MPW has a higher possibility of being economically competitive with fossil-based hydrogen. As the feedstock costs increase from US\$0 ODMT^{-1} to US\$136 ODMT^{-1}, the highest CCS cost that the MPW-derived hydrogen can tolerate decreases from US\$101 t^{-1} CO_2 to US\$53 t^{-1} CO_2 to hold the competitiveness with the current highest market price as US\$2.21 kg^{-1} fossil-based H_2 without CCS. The MHSP of Scenario 3-MPW ranges from US\$2.26 to 2.94 kg^{-1} H_2 (with \$0–\$151 ODMT^{-1} feedstock and \$105 t^{-1} CO_2 CCS cost). This MHSP range can compete with the price of fossil fuel hydrogen with CCS (US\$1.21–2.62 kg^{-1} H_2 (refs. [15,31,50–54])) or biomass-derived hydrogen (US\$0.73–3.17 kg^{-1} H_2 (refs. [31,55,56])), and is lower than the cost of current electrolysis hydrogen (US\$3.20–7.70 kg^{-1} H_2 (refs. [31,50,57])). With lower feedstock and CCS costs, the lowest MHSP that MPW can achieve is US\$1.59 kg^{-1} H_2 (with \$0 ODMT feedstock and \$53 t^{-1} CO_2), which is close to the mean value of the current hydrogen price. This result highlights the importance of policy support for ensuring the economic viability of utilizing MPW for hydrogen production coupled with CCS. According to the study

**Parameter (Optimistic, Baseline, Pessimistic, Unit)**
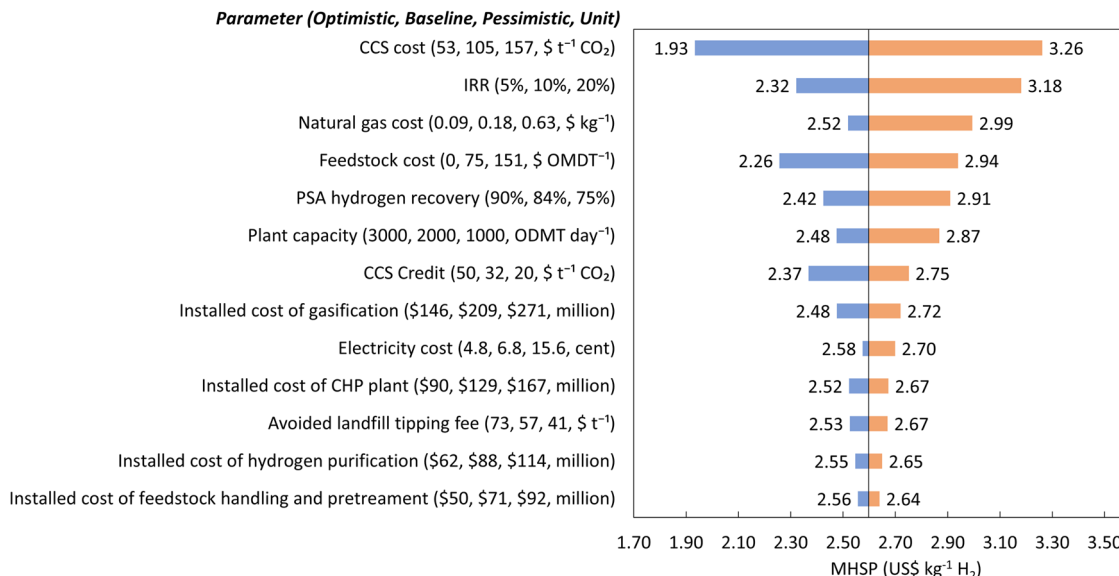
Fig. 4 Sensitivity analysis of Scenario 3-MPW at 2000 oven-dry metric tons per day. The blue bars indicate the optimistic results of MHSP due to parameter uncertainty, while the orange bars show pessimistic results.

by Milbrandt et al.[44], there are around 37.7 Mt of plastic waste in municipal solid waste (including durable goods, nondurable goods, containers, and packaging) ending in the U.S. landfills in 2019 (ref. [44]). Based on the result of this study, if 50% (a conservative estimation percentage[7]) of these landfilled MPW can be utilized for hydrogen production, around 4.1 Mt of hydrogen can be produced. This is equivalent to 41% of current annual hydrogen consumption (10 Mt per year in 2020) and approximately 10–19% of the estimated hydrogen demand by 2050 in the U.S. (22–41 Mt year^{-1})[44].

Sensitivity analysis of MHSP. Figure 4 shows the sensitivity analysis results of MHSP for Scenario 3-MPW at 2000 ODMT per day. The baseline MHSP in Fig. 4 is US$2.60 kg^{-1} H$_2$. The parameters with less than 2% impact when varying ±50% are not included. The rest of parameters were varied based on the data collected from the literature (see Supplementary Table 4). The lower and upper bounds of variations are shown within the parenthesis as optimistic and pessimistic values. CCS cost is the most impactful parameter, followed by Internal Rate of Return (IRR), natural gas cost, feedstock cost, pressure swing adsorption (PSA), hydrogen recovery efficiency, plant capacity, and carbon credits (larger than 5% impacts). This emphasizes the necessity of lowering the CCS cost for producing cost-competitive and low-carbon hydrogen from MPW. The natural gas cost in the U.S. varies by time and states. For example, in Connecticut, the industrial price of natural gas was US$5.88 per thousand cubic feet (MCF) in November 2019 and US$7.54 MCF^{-1} in March 2019, while in California, the price was US$7.16 MCF^{-1} in November 2019 and US$9.01 MCF^{-1} in March 2019[58]. The range of natural gas prices in Fig. 4 is the lowest and highest monthly price for industrial natural gas across the continental U.S. states in 2019[58]. Feedstock cost variation leads to ±13% change in the MHSP results. Increasing PSA recovery efficiency from 84% to 90% reduces the MHSP from US$2.60 to US$2.42 kg^{-1} H$_2$ by increasing the H$_2$ yield[15,59–62]. Decreasing carbon credit from $32 to $20 t^{-1} CO$_2$ increases $0.15 kg^{-1} H$_2$, while increasing carbon credits from $32 to $50 t^{-1} CO$_2$ (refs. [63–65]) decreases 0.23 kg^{-1} H$_2$. This range was developed based on the 45Q carbon credit that had the lowest $20 t^{-1} CO$_2$ in 2020 and is expected to reach US$50 t^{-1} CO$_2$ by 2026 (ref. [65]). This study only considers 45Q

carbon credits, however, more carbon credits could be available in the future by various policy and market mechanisms. Besides these parameters, other parameters related to material and energy cost (i.e., landfill tipping fee and electricity cost) and equipment cost have lower impacts on MHSP.

Roadmap to improve the economic feasibility. The sensitivity analysis identifies the driving factors of MHSP, such as CCS cost, PSA hydrogen recovery efficiency, IRR, and carbon credit. Based on the sensitivity analysis results, this study conducted an improvement analysis to exhibit a potential roadmap for the future development of waste-to-hydrogen pathways[19,22]. IRR is not included as it reflects the economic performance expectation. In Fig. 5, eleven parameters are listed in the descending order of effects (from largest to smallest) on MHSP in the sensitivity analysis. Figure 5 displays two pathways. The first one (light blue) shows the improvement based on the current best practices. In this pathway, the MHSP of Scenario 3-MPW can be reduced from US$2.60 to US$1.46 kg^{-1} H$_2$. The second pathway (light orange) is a more ambitious exploration to achieve the target of US$1.0 per kg of clean hydrogen in one decade set by the U.S. DOE[66]. In the second pathway, the CCS cost (decreasing to US$53 t^{-1} CO$_2$), carbon credits (increasing to US$50 t^{-1} CO$_2$), and feedstock cost (decreasing to US$38 ODMT^{-1} by 50% reduction) were assumed to reach the limit of data collected. Compared to the first pathway, CCS cost in the second pathway is much lower due to expected large technology improvement and optimization (e.g., CCS technology improvement, expanding capacity and reduced cost of geo-storage, optimizing CCS transport and storage network configuration), and high carbon credits (e.g., achieving the upper bound of 45Q by 2026[63–65]). The second pathway also has a huge reduction of feedstock cost when the avoided landfill tipping fee is high. Under this situation, the final MHSP can be as low as US$1.06 kg^{-1} H$_2$, indicating the necessity of strong policy in encouraging recycling and discouraging landfilling. The specific opportunities for each parameter were identified through a comprehensive literature review and listed in Supplementary Table 5. These opportunities shed light on future directions for more cost-effective conversion of plastic wastes into low-carbon hydrogen.
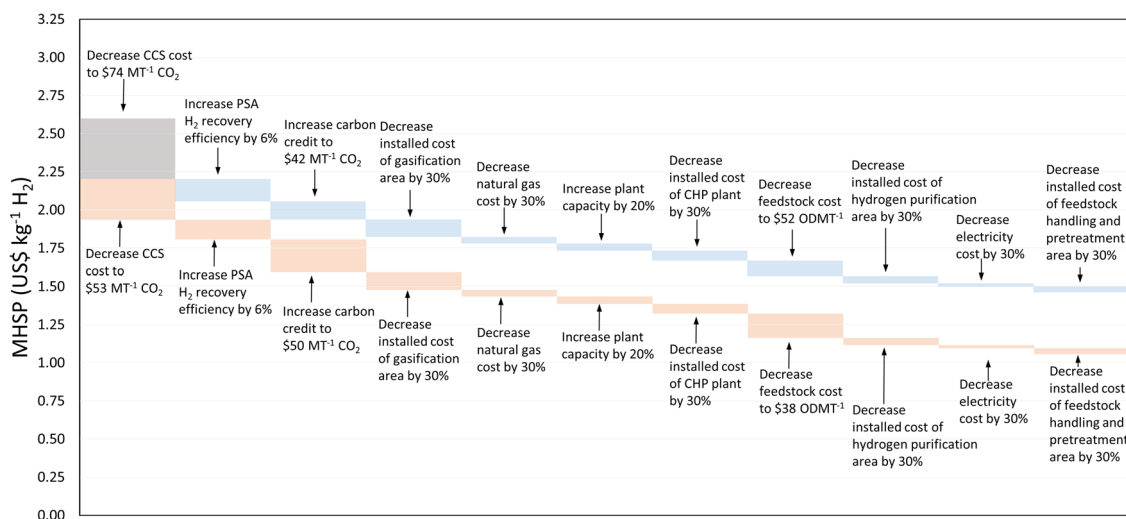
Fig. 5 Improvement analysis of Scenario 3-MPW at 2000 oven-dry metric tons per day under two pathways. The shaded box areas in each pathway display the cost reduction potential of improving each parameter. The gray area of the first bar represents the overlaps between the first and second pathways. Eleven parameters identified by the sensitivity analysis as the major drivers of economic feasibility were evaluated by their potential to be improved by current state-of-the-art practices (blue) or future advancement (orange). Detailed improvement measures for each parameter are provided in Supplementary Table 5. Detailed data of MHSP for each measure are in Supplementary Table 6.

Environmental impacts of plastic waste derived hydrogen. This study conducted the LCA to examine the environmental impacts of waste plastic-derived hydrogen. Figure 6 shows the normalized LCA results of ten impact categories in varied scenarios and feedstock cases under the optimal S/F ratios identified in Fig. 2. The LCA results of each impact category are normalized based on the highest value (on 1 kg H_2 basis) of that impact across Scenario 1–3 (including 5 feedstock cases in Scenario 1 without CCS and 5 feedstock cases in Scenario 2 & 3 with CCS). The absolute values of LCA results are in Supplementary Tables 7 and 8 in Supplementary Data 1 (ref. [67]).

In Fig. 6, MPW shows the lowest environmental impacts across all scenarios and impact categories (1–93% lower than the other four single-stream feedstocks) mainly due to the lower environmental burdens of feedstock collection, sorting (for single-stream cases), and transportation. Note that the burdens of producing plastic are assumed to be cut-off from the system boundary. Across most impact categories, feedstock collection, sorting, and transportation dominate the environmental impacts of hydrogen derived from single-stream plastic (27–94%), but they only contribute to 1–10% for MWP. The only exceptions are GWP and fossil fuel depletion that are dominated by energy, contributing to similar percentages of results for single-stream plastics and MPW (25–90%). MPW has 1–59% higher environmental burdens of chemicals and materials than that of PE, PP, and PS, given the additional steps in pretreatment and dechlorination. However, chemicals and materials overall only contribute to 1–32% of life cycle environmental impacts across all single-stream plastic feedstocks. Waste treatment has minor contributions to most impact categories except acidification and human health—carcinogenics, although MPW has 19–94% higher environmental burdens related to waste treatment than single-stream plastics. This is caused by the higher wastewater generation in pretreatment and dechlorination. Across single-stream plastics, PET shows the worst environmental performance, similar to TEA results for similar reasons – low hydrogen yields and high cost (environmental burdens) of sorting and processing plastic feedstock.

Adding CCS to the hydrogen plant increase all environmental impacts by 9–117% except reducing GWP by 42–67%, regardless of plastic feedstocks. The increased environmental impacts are attributed to the chemicals and energy consumption[68,69], while the decreased GWP are contributed by CCS that removes carbon.

From the perspective of climate change, MPW-derived hydrogen without CCS has higher life cycle GWP (16.0–21.0 kg CO_2e kg^{-1} H_2, depending on S/F ratios, see Supplementary Table 9 for detailed values) than natural gas (9.0–12.3 kg CO_2e kg^{-1} H_2 (refs. [15,51,52,54,70])) but mostly lower than coal (20.0–26.0 kg CO_2e kg^{-1} H_2 (refs. [51-54])). CCS reduces the GWP of MPW-derived hydrogen to 5.1–6.2 kg CO_2e kg^{-1} H_2, which is much lower than fossil-based hydrogen without CCS. However, if CCS is implemented for fossil-based hydrogen in the future, MPW-derived hydrogen will have higher life-cycle GWP than natural gas-based hydrogen with CCS (1.0–4.1 kg CO_2e kg^{-1} H_2 (refs. [15,31,51])), and comparable with coal-based hydrogen with CCS (2.0–6.9 kg CO_2e kg^{-1} H_2 (refs. [51-54])) or biomass gasification hydrogen without CCS (0.3–19.2 kg CO_2e kg^{-1} H_2 (refs. [31,71-73])). MPW-derived hydrogen with CCS has lower life-cycle GWP than electrolysis hydrogen from global average grid electricity (25.5 kg CO_2e kg^{-1} H_2 (ref. [51])), although the GWP of MPW-derived hydrogen with CCS is higher than electrolysis hydrogen with clean electricity (0.9–6.9 kg CO_2e kg^{-1} H_2 (refs. [70,71])), or biomass gasification with CCS (−18.8 to −9.6 kg CO_2e kg^{-1} H_2 (refs. [31,71])). As most GHG emissions are attributed to energy consumption (Fig. 6b), future research should focus on improving energy efficiency and exploring alternative energy sources to reduce the life cycle GWP of MPW-derive hydrogen.

For other impact categories, this study compared Scenario 3-MPW with CCS with hydrogen made from natural gas using steam reforming and CCS (see Supplementary Fig. 12). The MPW with CCS is 2.4–80.3% lower than natural gas with CCS in acidification, fossil fuel depletion, ozone depletion, and smog formation. At the same time, hydrogen from natural gas with CCS is 26.8–53.6% lower than Scenario 3-MPW with CCS in carcinogenics, non-carcinogenics, ecotoxicity, eutrophication, and respiratory effects.

Discussion

This study conducted a TEA and LCA to explore the economic feasibility and environmental performance of hydrogen production
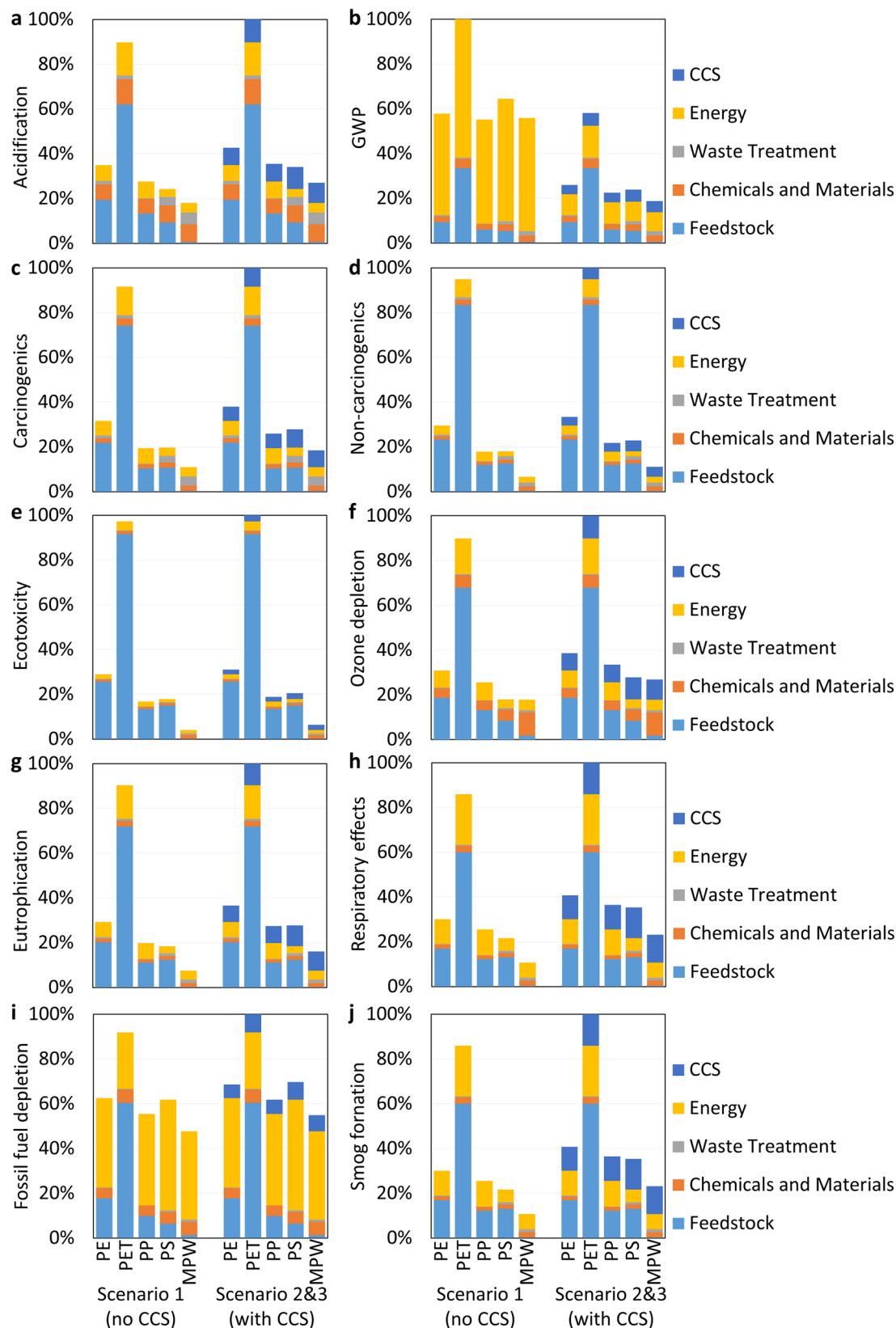
Fig. 6 Normalized Life Cycle Assessment results of five cases with and without carbon capture and storage. a acidification; **b** Global Warming Potential **c** carcinogenics (human health); **d** non-carcinogenics (human health); **e** ecotoxicity; **f** ozone depletion; **g** eutrophication; **h** respiratory effects; **i** fossil fuel depletion; **j** smog formation. Scenario 1 does not have CCS; Scenarios 2 and 3 have CCS and the same LCA results (as the difference is the inclusion/exclusion of carbon credits that affect TEA but not LCA). The results are decomposed into five contributors. The LCA results of 1 kg H₂ in each impact category are normalized based on the largest result across Scenarios 1–3.

from gasifying MPW that commonly ends in landfill. The TEA and LCA were coupled with the process simulation model developed in Aspen Plus to determine the impacts of plant capacities, feedstock compositions, policy incentives, and process parameters on MHSP and life-cycle environmental impacts. It is economically feasible to produce US$1.67 kg^{-1} H$_2$ from a 2000 ODMT per day hydrogen plant utilizing MPW without CCS, compared with the current fossil-based hydrogen price without CCS (US$0.91–$2.21 kg^{-1} H$_2$). Incorporating CCS into the gasification plant increases most environmental impacts due to the additional chemical and energy consumption of CCS systems. The only exception is GWP given the carbon removal benefits of CCS. Adding CCS also increases the MHSP to US$2.60 kg^{-1} H$_2$ (US$2.26–$2.94 kg^{-1} upon varied feedstock cost) for the same plant, and the economic feasibility of a CCS-coupled hydrogen plant depends on CCS cost and policy incentives. CCS is essential to ensure that MPW-derived hydrogen has lower life cycle GHG emissions than current fossil-based hydrogen, and this advantage may not hold if CCS is implemented for natural gas-based hydrogen in the future. Future research is needed to reduce energy-related carbon emissions to lower the life cycle GWP of MPW-derived hydrogen. The results show the economic and environmental advantages of using MPW over single-stream plastics (i.e., PE, PET, PP, and PS) in producing hydrogen via gasification, given the high feedstock cost and environmental burdens of sorting and processing single-stream plastics in MRFs at current stage and low hydrogen yield of some plastics (e.g., PET). Given the current high portion of MPW landfilled or discarded, more efforts are needed to prioritize MPW valorization in an environmentally benign and cost-effective way. Among single-stream plastics, PET is the least favorable in terms of both environmental and economic performance. This implies the necessity of exploring other high-value and feasible recycling methods for sorted single-stream plastics (e.g., replacing virgin materials)[7]. Increasing the plant capacity can reduce the MHSP across all feedstock cases. From an operational aspect, the steam/feed ratio directly affects MHSP, and the optimal steam/feedstock ratio varies by feedstock (e.g., 2.0 for MPW and 3.5 for PS) and generally increases as the feedstock cost grows. The improvement analysis exhibits possible pathways to decrease the MHSP of MWP-derived hydrogen with CCS from US$2.60 to US$1.46 kg^{-1} H$_2$. If carbon credits are close to the CCS costs and MPW feedstock cost is low, the MHSP of utilizing MPW can reach US$1.06 kg^{-1} H$_2$. To achieve the ambitious goal of US$1.0 per kg clean hydrogen in one decade, the roadmap highlights the need for simultaneous improvement of process economics and policy supports.

Methods

Feedstock compositions. Common plastic wastes include PET, high-density polyethylene (HDPE), PVC, low-density polyethylene (LDPE), PP, PS, and other plastic waste[39,74]. Supplementary Table 2 summarizes the composition data from the proximate and ultimate analysis of the plastics used in this study. Five feedstock cases were developed to investigate the impacts of different plastic waste feeds, particularly to compare the economic and environmental performance of single-stream plastic feed and MPW. Four cases use single-stream plastic waste, including PE (assuming 50% LDPE and 50% HDPE), PET, PP, and PS provided by sorting or recycling facilities. Pure PVC feed was not selected due to extremely high chlorine content causing safety and corrosion concerns[75]. One case was designed for MPW that was typically rejected from the mechanical recycling at MRF[7]. These MPW are commonly landfilled that need "tipping fee" or incinerated to generate power[7,76]. In this study, MPW contains 19.5% HDPE, 27.9% LDPE, 27.5% PP, 7.6% PS, 14.6% PET, and 2.9% PVC based on the data of landfilled plastic waste that is neither recycled nor combusted in the U.S. in the year 2018 by U.S. EPA[76].

Process simulation model of the hydrogen plant. A process simulation model was established in Aspen Plus to provide mass and energy data for TEA and LCA[32]. As shown in Fig. 1, the hydrogen plant comprises five main areas: feedstock handling and pretreatment, gasification, hydrogen purification, CHP plant, and utilities. The detailed process diagrams of Aspen Plus in each area are shown in Supplementary Figs. 13–17. An example of summarized flow information is

available in Supplementary Fig. 18 and Supplementary Table 10 in Supplementary Data 1 (ref. [67]).

In this study, five different feedstocks (i.e., PE, PET, PP, PS, and MPW as shown in Supplementary Table 1) were fed into the simulation model to study the impacts of varied feedstock compositions. The plastic waste is assumed to arrive at the hydrogen plant in the form of bales[7,77]. The bales are then unloaded and transferred to the warehouse for storage. The first unit operation is the size reduction of the plastic waste in the shredder to around 152 mm (6 inches)[78]. After the initial grinding, the feedstocks are washed in the rotary drum washer to remove the entrained ash and other contaminates[7,79,80]. Different from the pure feedstocks (i.e., PE, PET, PP, PS) that have been sorted and processed, MPW will undergo two washing steps in friction washers as a common practice[7]. Then the feedstocks are dried in the rotary drum dryer at 105 °C to reach a moisture content lower than 10% (dry basis)[81,82]. Followed by drying, feedstocks are further grounded in the secondary grinding to around 1–2 mm[7,81], and are ready for gasification.

Before gasification, dechlorination is essential for removing toxic chlorine from PVC for safety and corrosion concerns. Based on the study by López et al., treating the plastic mixtures containing PVC at 300 °C in a nitrogen atmosphere for 30 min can efficiently remove 99.2% of chlorine in PVC[75]. In this study, the dechlorination process is conducted at the same condition before gasification[75,83]. The weight loss of PE, PP, PS, and PET in the dechlorination process is only 0.7%, 0.3%, 3.3%, and 0.8%, respectively[75]. Two-stage gasification was modeled in this study, including gasification followed by tar cracking which is essential for large-scale hydrogen plant operation[84]. This study uses a bubbling fluidized bed reactor for gasification, and a fixed bed reactor for tar cracking based on the literature[84,85]. For gasification, the operating condition was selected to be 850 °C and 3.5 MPa with steam as the gasifying agent for H$_2$-rich production[13,86,87]. In Aspen Plus, the gasification was modeled with two reactors in sequence using RStoic and RGibbs, which is consistent with previous process simulations for gasification[40,88–93]. The RStoic reactor decomposes the inlet stream based on the feedstock compositions. Then the decomposed stream along with steam is sent to the RGibbs reactor that calculates the syngas composition using Gibbs free energy minimization method[88,89]. In RGibbs reactor, 12 reactions are considered based on the literature (see Supplementary Table 11 for detailed reactions)[94–96].

This study uses steam gasification which is commonly used for generating H$_2$-rich syngas as the presence of steam can increase hydrogen yield, reduce the tar concentration, and promote water gas shift reactions[85,97–100]. Previous studies show the importance of S/F ratio in gasification design and optimization[40]. The S/F ratio commonly varies from 1.0 to 4.0[40,85]. The higher S/F ratio may lead to higher hydrogen yield, but at the same time can cause higher energy cost. To choose a suitable S/F ratio, this study investigated the S/F ratios from 1.0 to 4.0 in each feedstock case, and selected the S/F ratio with the lowest MHSP. The bed material is natural olivine with a diameter of 100–300 μm[37,84]. Natural olivine is a highly attrition-resistant catalyst to reduce tar formation[37,84]. For tar cracking, the fixed bed reactor operates at 800 °C and 3.5 MPa with additives that are 1:1.5 mixtures of calcined dolomite and activated carbon[84]. These additives can efficiently decompose the NH$_3$ formed in gasification and reduce the concentration of HCl and H$_2$S in syngas[84]. After the tar cracking, a cyclone is deployed to separate the solid phase (e.g., fly ash)[101].

After the hot syngas is generated, the first step is to remove the impurities. The moving-bed granular filter with CaO is deployed to desulfurize and dechlorinate the hot syngas[102,103]. Then the remaining tar is removed by a Venturi scrubber at about 35 °C and a wet-packed column for fine tar removal[101,104]. To integrate the tar removing with other impurity removing, the Venturi scrubber washes with 10% NaOH solution to remove the remaining HCN, HCl, and H$_2$S[105,106]. To further eliminate NH$_3$, an acid wash column with H$_2$SO$_4$ solution at pH 5 is adopted[107]. The purified gas primarily contains H$_2$, H$_2$O, CO, CO$_2$, and CH$_4$. To separate hydrogen, the syngas is compressed to 13.7 atm and fed to a PSA which is assumed 84% hydrogen recovery with 99% purity[106]. All the off-gases are sent to the CHP plant for energy recovery[106]. To store the hydrogen, the purified hydrogen is assumed to be compressed to 700 bars through two-stage compressing[108]. 700 bar is a common pressure level for storage or for hydrogen stations to refuel the fuel cell[108,109].

As this study uses steam gasification, the steam load in the gasification area is high. At the same time, the hydrogen plant consumes electricity in each area. Given the demand of electricity and heat, this study includes a CHP plant that recovers the energy in PSA off-gas and char to produce electricity and heat needed by the whole plant. If the heat supply is not sufficient by combusting the intermediate flows, natural gas will be combusted as a supplementary fuel. The boiler generates superheated steam at 62 atm and 454 °C with 80% boiler energy efficiency[110]. The superheated steam then goes through multi-stage turbines for power generation. In this study, the low-pressure steam at 13 atm and 268 °C from the first stage turbine is extracted for feeding the gasifier and providing heat to the dechlorination reactor and tar cracking reactor.

Plant utilities include electricity, cooling water, process water, chilled water, plant air system, and the storage of materials and products[110,111]. All of these utilities are included in the process simulation, TEA, and LCA.

This study includes scenarios with and without CCS. CCS captures and stores the CO$_2$ from the CHP plant flue gas. The CO$_2$ concentration in the cooled flue gas

is around 23 vol.%. Post-combustion CCS was chosen because of its suitableness for capturing carbon from air-combusted flue gas with much lower CO_2 concentration (commonly lower than 25 vol. % of flue gas[112,113]) than oxyfuel combustion CCS that uses pure O_2 (ref. [114]). The capture efficiency is assumed to be 90% for post-combustion CCS[115]. See Supplementary Note 5 for detailed technical information and Supplementary Note 4 for cost data.

Techno-economic analysis model. This study focuses on the hydrogen plant with a capacity of 100–2000 ODMT plastic waste per day. The mass and energy balance data by Aspen Plus simulation were input to determine variable operating costs and capital costs. In TEA, the original purchased costs, installing factors, equipment scaling factors, and material and energy prices, and feedstock costs were collected from the literature and discussed in Supplementary Note 6 for capital expenditures and Supplementary Note 4 for operating expenditures. The MHSP, a widely adopted indicator describing the production cost under preset IRR, was selected to assess the economic feasibility of the hydrogen plant[33]. The MHSP was derived through the discounted cash flow rate of return (DCFROR) analysis as a widely used economic analysis method in TEA[23]. In the DCFROR analysis established in EXCEL, the MHSP was derived by setting the IRR to be 10% and the Net Present Value (NPV) to be zero[23]. The year of analysis is 2019 based on the latest data availability. Supplementary Tables 12 and 13 list the key assumptions and parameters of TEA based on literature data. The plant is assumed to have 40% equity-financed and take the remaining 60% on loan. The capital cost was assumed to be depreciated over 7 years by following the Modified Accelerated Cost Recovery System by the U.S. IRS[116].

The total capital investment includes total installed equipment cost, other direct costs, indirect cost, and land and working capital. Total installed equipment cost is the sum of the installed equipment costs that were estimated by multiplying purchased costs with installation factors (see Supplementary Tables 14–18). The purchased costs and installation factors used in this study were collected from the literature as shown in Supplementary Note 6. The economy of scale was considered using the scaling factors (see Supplementary Note 6) to scale the purchased costs found in the literature to the capacities explored in this study. Plant cost indices by Chemical Engineering Magazine were used[117] to adjust equipment purchased costs collected from the literature to the year of analysis 2019 in this study. The detailed method of determining equipment cost is documented in Supplementary Note 6.

The operating expenditures include the variable costs of feedstocks, raw materials, waste stream charges, byproduct credits, and fixed operating costs (including labor cost), and other operating costs. The prices of feedstocks, raw materials, waste stream charges, and energy were collected from the literature and documented in Supplementary Table 3. If the price is not in the year of analysis (2019), the Producer Price Index for chemical manufacturing was used to adjust the original prices to 2019 (ref. [118]). The details are available in Supplementary Note 4 and Supplementary Table 19.

Life cycle assessment model. In this study, a cradle-to-gate LCA was conducted to display the environmental impacts of hydrogen converted from MPW. The life cycle inventory (LCI) data for the hydrogen plant were derived from the Aspen Plus simulation for different scenarios, including energy and material consumption (e.g., fuels, chemicals, water) and CHP plant emissions. AP-42 emission factors by U.S. EPA were used to estimate emissions from natural gas combustion (see Supplementary Table 20 for emission factors)[119]. The LCI data of upstream production of electricity and materials and treatment of wastewater and solid waste (e.g., ash) were collected from the ecoinvent database (see Supplementary Table 21 for the unit processes used in this study)[120]. The functional unit is 1 kg H_2 produced in consistency with the TEA. LCIA uses the TRACI 2.1 method by U.S. EPA and 100-year GWP characterization factors by IPCC AR6 2021[34,35].

Data availability
The authors declare that all data supporting the results of this study are available within the article, corresponding Supplementary Information (Supplementary Notes 1–6, Supplementary Tables 1–6, 9, and 11–21), and Supplementary Data (Supplementary Tables 1–21 in Supplementary Data 1) that have been deposited and are publicly available on Zenodo (https://doi.org/10.5281/zenodo.7275343).

Code availability
No computer code that was central to the results was programmed in preparing the paper. The process simulation was performed in Aspen Plus V11 (37.0.0.395). The TEA was fully performed in Microsoft Excel (version 2201). The LCA was performed in OpenLCA 1.10.3 (Windows 64 bit) and Microsoft Excel (version 2201).

References
1. Geyer, R., Jambeck, J. R. & Law, K. L. Production, use, and fate of all plastics ever made. *Sci. Adv.* **3**, 25–29 (2017).
2. Thomas, K. V. Understanding the plastics cycle to minimize exposure. *Nat. Sustain.* **5**, https://doi.org/10.1038/s41893-021-00814-3 (2021).
3. Sun, J. et al. Revisiting microplastics in landfill leachate: unnoticed tiny microplastics and their fate in treatment works. *Water Res.* **190**, 116784 (2021).
4. Xia, Q. et al. A strong, biodegradable and recyclable lignocellulosic bioplastic. *Nat. Sustain.* **4**, 627–635 (2021).
5. Ganesh Kumar, A., Anjana, K., Hinduja, M., Sujitha, K. & Dharani, G. Review on plastic wastes in marine environment—Biodegradation and biotechnological solutions. *Mar. Pollut. Bull.* **150**, 110733 (2020).
6. Chae, Y. & An, Y. J. Current research trends on plastic pollution and ecological impacts on the soil ecosystem: A review. *Environ. Pollut.* **240**, 387–395 (2018).
7. Ragaert, K., Delva, L. & Van Geem, K. Mechanical and chemical recycling of solid plastic waste. *Waste Manag.* **69**, 24–58 (2017).
8. Triebert, D., Hanel, H., Bundt, M. & Wohnig, K. Solvent-based recycling. in *Circular Economy of Polymers: Topics in Recycling Technologies* 33–59 (American Chemical Society, 2021). https://doi.org/10.1021/bk-2021-1391.ch003.
9. Hahladakis, J. N. & Iacovidou, E. An overview of the challenges and trade-offs in closing the loop of post-consumer plastic waste (PCPW): Focus on recycling. *J. Hazard. Mater.* **380**, 120887 (2019).
10. Qureshi, M. S. et al. Pyrolysis of plastic waste: Opportunities and challenges. *J. Anal. Appl. Pyrolysis* **152**, 104804 (2020).
11. Carey, J. On the brink of a recycling revolution? *Proc. Natl. Acad. Sci.* **114**, 612–616 (2017).
12. Dogu, O. et al. The chemistry of chemical recycling of solid plastic waste via pyrolysis and gasification: State-of-the-art, challenges, and future directions. *Prog. Energy Combust. Sci.* **84**, 100901 (2021).
13. Salaudeen, S. A., Arku, P. & Dutta, A. Gasification of plastic solid waste and competitive technologies. In Plastics to Energy: Fuel, Chemicals, and Sustainability Implications (Elsevier Inc., 2019). https://doi.org/10.1016/B978-0-12-813140-4.00010-8.
14. Chai, Y., Gao, N., Wang, M. & Wu, C. H_2 production from co-pyrolysis/gasification of waste plastics and biomass under novel catalyst Ni-CaO-C. *Chem. Eng. J.* **382**, 122947 (2020).
15. Khojasteh Salkuyeh, Y., Saville, B. A. & MacLean, H. L. Techno-economic analysis and life cycle assessment of hydrogen production from natural gas using current and emerging technologies. *Int. J. Hydrogen Energy* **42**, 18894–18909 (2017).
16. McQueen, S. et al. Department of Energy Hydrogen Program Plan. *U.S. Department of Energy* https://www.hydrogen.energy.gov/pdfs/hydrogen-program-plan-2020.pdf (2020).
17. Wu, C. & Williams, P. T. Pyrolysis-gasification of plastics, mixed plastics and real-world plastic waste with and without Ni-Mg-Al catalyst. *Fuel* **89**, 3022–3032 (2010).
18. Rosa, L., Reimer, J. A., Went, M. S. & D'Odorico, P. Hydrological limits to carbon capture and storage. *Nat. Sustain.* **3**, 658–666 (2020).
19. Shin, H., Hansen, K. U. & Jiao, F. Techno-economic assessment of low-temperature carbon dioxide electrolysis. *Nat. Sustain.* **4**, 911–919 (2021).
20. Stolz, B., Held, M., Georges, G. & Boulouchos, K. Techno-economic analysis of renewable fuels for ships carrying bulk cargo in Europe. *Nat. Energy* **7**, 203–212 (2022).
21. Yu, Z. J., Carpenter, J. V. & Holman, Z. C. Techno-economic viability of silicon-based tandem photovoltaic modules in the United States. *Nat. Energy* **3**, 747–753 (2018).
22. Lan, K. et al. Techno-economic analysis of producing xylo-oligosaccharides and cellulose microfibers from lignocellulosic biomass. *Bioresour. Technol.* **340**, 125726 (2021).
23. Lan, K. et al. Techno-economic analysis of decentralized preprocessing systems for fast pyrolysis biorefineries with blended feedstocks in the Southeastern United States. *Renew. Sustain. Energy Rev.* **143**, 110881 (2021).
24. Lan, K. et al. Impacts of uncertain feedstock quality on the economic feasibility of fast pyrolysis biorefineries with blended feedstocks and decentralized preprocessing sites in the Southeastern United States. *GCB Bioenergy* **12**, 1014–1029 (2020).
25. ISO. ISO 14044: Environmental Management, Life Cycle Assessment, Requirements, and Guidelines. https://www.iso.org/standard/38498.html, (2006).
26. Lan, K. & Yao, Y. Dynamic life cycle assessment of energy technologies under different greenhouse gas concentration pathways. *Environ. Sci. Technol.* **56**, 1395–1404 (2022).
27. Lan, K. et al. Dynamic life-cycle carbon analysis for fast pyrolysis biofuel produced from pine residues: implications of carbon temporal effects. *Biotechnol. Biofuels* **14**, 1–17 (2021).
28. Lan, K. & Yao, Y. Integrating life cycle assessment and agent-based modeling: a dynamic modeling framework for sustainable agricultural systems. *J. Clean. Prod.* **238**, 117853 (2019).

29. Lan, K., Zhang, B. & Yao, Y. Circular utilization of urban tree waste contributes to the mitigation of climate change and eutrophication. *One Earth* 1–14. https://doi.org/10.1016/j.oneear.2022.07.001 (2022).

30. Lan, K., Kelley, S. S., Nepal, P. & Yao, Y. Dynamic life cycle carbon and energy analysis for cross-laminated timber in the Southeastern United States. *Environ. Res. Lett.* **15**, 124036 (2020).

31. Wu, N., Lan, K. & Yao, Y. An integrated techno-economic and environmental assessment for carbon capture in hydrogen production by biomass gasification. *Resour. Conserv. Recycl.* **188**, 106693 (2023).

32. AspenTech. *Aspen Plus 11.1 User Guide.* https://www.aspentech.com/en/products/engineering/aspen-plus (2020).

33. Tao, L., Markham, J. N., Haq, Z. & Biddy, M. J. Techno-economic analysis for upgrading the biomass-derived ethanol-to-jet blendstocks. *Green Chem.* **19**, 1082–1101 (2017).

34. Forster, P. et al. The Earth's Energy Budget, Climate Feedbacks, and Climate Sensitivity. In Climate Change 2021: The Physical Science Basis. Contribution of Working Group I to the Sixth Assessment Report of the Intergovernmental Panel on Climate Change (Cambridge University Press, Cambridge, United Kingdom and New York, NY, USA, 2021). https://doi.org/10.1017/9781009157896.009.

35. Ryberg, M., Vieira, M. D. M., Zgola, M., Bare, J. & Rosenbaum, R. K. Updated US and Canadian normalization factors for TRACI 2.1. *Clean Technol. Environ. Policy* **16**, 329–339 (2014).

36. Midilli, A., Kucuk, H., Haciosmanoglu, M., Akbulut, U. & Dincer, I. A review on converting plastic wastes into clean hydrogen via gasification for better sustainability. *Int. J. Energy Res.* **46**, 4001–4032 (2022).

37. Sancho, J. A., Aznar, M. P. & Toledo, J. M. Catalytic air gasification of plastic waste (Polypropylene) in fluidized bed. Part I: Use of in-gasifier bed additives. *Ind. Eng. Chem. Res.* **47**, 1005–1010 (2008).

38. Santagata, C. et al. Production of low-density poly-ethylene (LDPE) from chemical recycling of plastic waste: Process analysis. *J. Clean. Prod.* **253**, 119837 (2020).

39. Anuar Sharuddin, S. D., Abnisa, F., Wan Daud, W. M. A. & Aroua, M. K. A review on pyrolysis of plastic wastes. *Energy Convers. Manag.* **115**, 308–326 (2016).

40. Saebea, D., Ruengrit, P., Arpornwichanop, A. & Patcharavorachot, Y. Gasification of plastic waste for synthesis gas production. *Energy Reports* **6**, 202–207 (2020).

41. Susastriawan, A. A. P., Purnomo & Sandria, A. Experimental study the influence of zeolite size on low-temperature pyrolysis of low-density polyethylene plastic waste. *Therm. Sci. Eng. Prog.* **17**, 100497 (2020).

42. Janajreh, I., Adeyemi, I. & Elagroudy, S. Gasification feasibility of polyethylene, polypropylene, polystyrene waste and their mixture: Experimental studies and modeling. *Sustain. Energy Technol. Assessments* **39**, 100684 (2020).

43. Williams, P. T. & Slaney, E. Analysis of products from the pyrolysis and liquefaction of single plastics and waste plastic mixtures. *Resour. Conserv. Recycl.* **51**, 754–769 (2007).

44. Milbrandt, A., Coney, K., Badgett, A. & Beckham, G. T. Quantification and evaluation of plastic waste in the United States. *Resour. Conserv. Recycl.* **183**, 106363 (2022).

45. Heikkinen, J. M., Hordijk, J. C., De Jong, W. & Spliethoff, H. Thermogravimetry as a tool to classify waste components to be used for energy generation. *J. Anal. Appl. Pyrolysis* **71**, 883–900 (2004).

46. Hundertmark, T., Prieto, M., Ryba, A., Simons, T. J. & Wallach, J. *Accelerating plastic recovery in the United States.* https://www.mckinsey.com/industries/chemicals/our-insights/accelerating-plastic-recovery-in-the-united-states (2019).

47. Masanet, E. & Horvath, A. Assessing the benefits of design for recycling for plastics in electronics: A case study of computer enclosures. *Mater. Des.* **28**, 1801–1811 (2007).

48. Dubanowitz, A. J. Design of a materials recovery facility (MRF) for processing the recyclable materials of New York City's municipal solid waste. Master thesis. (Columbia University, 2000).

49. Wu, G., Li, J. & Xu, Z. Triboelectrostatic separation for granular plastic waste recycling: A review. *Waste Manag.* **33**, 585–597 (2013).

50. International Energy Agency. Global average levelised cost of hydrogen production by energy source and technology, 2019 and 2050. https://www.iea.org/data-and-statistics/charts/global-average-levelised-cost-of-hydrogen-production-by-energy-source-and-technology-2019-and-2050 (2022).

51. International Energy Agency. The future of hydrogen seizing today's opportunities. https://www.iea.org/reports/the-future-of-hydrogen (2019).

52. Simons, A. & Bauer, C. Life cycle assessment of hydrogen production. Transition to Hydrogen: Pathways Toward Clean Transportation. https://doi.org/10.1017/CBO9781139018036.006 (2011).

53. Verma, A. & Kumar, A. Life cycle assessment of hydrogen production from underground coal gasification. *Appl. Energy* **147**, 556–568 (2015).

54. Jaramillo, P., Samaras, C., Wakeley, H. & Meisterling, K. Greenhouse gas implications of using coal for transportation: Life cycle assessment of coal-to-

55. Lepage, T., Kammoun, M., Schmetz, Q. & Richel, A. Biomass-to-hydrogen: A review of main routes production, processes evaluation and techno-economical assessment. *Biomass and Bioenergy* **144**, 105920 (2021).

56. Binder, M., Kraussler, M., Kuba, M. & Luisse, M. *Hydrogen from biomass gasification.* https://www.ieabioenergy.com/wp-content/uploads/2019/01/Wasserstoffstudie_IEA-final.pdf (2019).

57. IRENA. Green Hydrogen Cost Reduction: Scaling up Electrolysers to Meet the 1.5°C Climate Goal. (International Renewable Energy Agency). https://www.irena.org/publications/2020/Dec/Green-hydrogen-cost-reduction (2020).

58. US EIA. Natural Gas Prices. https://www.eia.gov/dnav/ng/NG_PRI_SUM_A_EPG0_PIN_DMCF_M.htm (2020).

59. Yáñez, M. et al. PSA purification of waste hydrogen from ammonia plants to fuel cell grade. *Sep. Purif. Technol.* **240**, 116334 (2020).

60. Davis, R. et al. *Process Design and Economics for the Conversion of Lignocellulosic Biomass to Hydrocarbons: Dilute-Acid and Enzymatic Deconstruction of Biomass to Sugars and Catalytic Conversion of Sugars to Hydrocarbons.* https://doi.org/10.1021/ed060p574 (2015).

61. Grande, C. A. Advances in pressure swing adsorption for gas separation. *ISRN Chem. Eng.* **2012**, 1–13 (2012).

62. Du, Z. et al. A review of hydrogen purification technologies for fuel cell vehicles. *Catalysts* **11**, 1–19 (2021).

63. Folger, P. *Carbon Capture and Sequestration (CCS) in the United States.* Congressional Research Service https://fas.org/sgp/crs/misc/R44902.pdf (2018).

64. Benson, S. M. & Deutch, J. Advancing enhanced oil recovery as a sequestration asset. *Joule* **2**, 1386–1389 (2018).

65. Congressional Research Service. The Tax Credit for Carbon Sequestration (Section 45Q). https://crsreports.congress.gov/product/pdf/IF/IF11455 (2021).

66. US DOE. Secretary Granholm Launches Hydrogen Energy Earthshot to Accelerate Breakthroughs Toward a Net-Zero Economy. https://www.energy.gov/articles/secretary-granholm-launches-hydrogen-energy-earthshot-accelerate-breakthroughs-toward-net (2021).

67. Lan, K. & Yao, Y. Supplementary Data 1. https://doi.org/10.5281/zenodo.7275343 (2022).

68. Zhang, X. et al. Post-combustion carbon capture technologies: Energetic analysis and life cycle assessment. *Int. J. Greenh. Gas Control* **27**, 289–298 (2014).

69. Budinis, S. et al. An assessment of CCS costs, barriers and potential. *Energy Strateg. Rev.* **22**, 61–81 (2018).

70. Cetinkaya, E., Dincer, I. & Naterer, G. F. Life cycle assessment of various hydrogen production methods. *Int. J. Hydrogen Energy* **37**, 2071–2080 (2012).

71. Al-Qahtani, A., Parkinson, B., Hellgardt, K., Shah, N. & Guillen-Gosalbez, G. Uncovering the true cost of hydrogen production routes using life cycle monetisation. *Appl. Energy* **281**, 115958 (2021).

72. Koroneos, C., Dompros, A. & Roumbas, G. Hydrogen production via biomass gasification-A life cycle assessment approach. *Chem. Eng. Process. Process Intensif.* **47**, 1261–1268 (2008).

73. Kalinci, Y., Hepbasli, A. & Dincer, I. Life cycle assessment of hydrogen production from biomass gasification systems. *Int. J. Hydrogen Energy* **37**, 14026–14039 (2012).

74. Abnisa, F. & Wan Daud, W. M. A. A review on co-pyrolysis of biomass: An optional technique to obtain a high-grade pyrolysis oil. *Energy Convers. Manag.* **87**, 71–85 (2014).

75. López, A., De Marco, I., Caballero, B. M., Laresgoiti, M. F. & Adrados, A. Dechlorination of fuels in pyrolysis of PVC containing plastic wastes. *Fuel Process. Technol.* **92**, 253–260 (2011).

76. US EPA. *Advancing sustainable materials management: facts and figures 2018.* United States Environmental Protection Agency. https://www.epa.gov/sites/default/files/2021-01/documents/2018_tables_and_figures_dec_2020_fnl_508.pdf (2020).

77. Aryan, Y., Yadav, P. & Samadder, S. R. Life Cycle Assessment of the existing and proposed plastic waste management options in India: A case study. *J. Clean. Prod.* **211**, 1268–1283 (2019).

78. Lan, K., Ou, L., Park, S., Kelley, S. S. & Yao, Y. Life cycle analysis of decentralized preprocessing systems for fast pyrolysis biorefineries with blended feedstocks in the Southeastern United States. *Energy Technol.* **1900850**. https://doi.org/10.1002/ente.201900850 (2019).

79. Aznar, M. P., Caballero, M. A., Sancho, J. A. & Francés, E. Plastic waste elimination by co-gasification with coal and biomass in fluidized bed with air in pilot plant. *Fuel Process. Technol.* **87**, 409–420 (2006).

80. Sogancioglu, M., Yel, E. & Ahmetli, G. Investigation of the Effect of Polystyrene (PS) waste washing process and pyrolysis temperature on (PS) Pyrolysis product quality. *Energy Procedia* **118**, 189–194 (2017).

81. Dong, J. et al. Effect of operating parameters and moisture content on municipal solid waste pyrolysis and gasification. *Energy and Fuels* **30**, 3994–4001 (2016).

82. Gug, J. I., Cacciola, D. & Sobkowicz, M. J. Processing and properties of a solid energy fuel from municipal solid waste (MSW) and recycled plastics. *Waste Manag.* **35**, 283–292 (2015).

83. Al-Salem, S. M., Antelava, A., Constantinou, A., Manos, G. & Dutta, A. A review on thermal and catalytic pyrolysis of plastic solid waste (PSW). *J. Environ. Manage.* **197**, 177–198 (2017).

84. Cho, M. H., Mun, T. Y., Choi, Y. K. & Kim, J. S. Two-stage air gasification of mixed plastic waste: Olivine as the bed material and effects of various additives and a nickel-plated distributor on the tar removal. *Energy* **70**, 128–134 (2014).

85. Alipour Moghadam Esfahani, R. et al. H2-rich syngas production through mixed residual biomass and HDPE waste via integrated catalytic gasification and tar cracking plus bio-char upgrading. *Chem. Eng. J.* **308**, 578–587 (2017).

86. Ozturk, M. & Dincer, I. An integrated system for clean hydrogen production from municipal solid wastes. *Int. J. Hydrogen Energy* **46**, 6251–6261 (2021).

87. Sara, H. R., Enrico, B., Mauro, V., Andrea, D. C. & Vincenzo, N. Techno-economic analysis of hydrogen production using biomass gasification -a small scale power plant study. *Energy Procedia* **101**, 806–813 (2016).

88. Tungalag, A., Lee, B. J., Yadav, M. & Akande, O. Yield prediction of MSW gasification including minor species through ASPEN plus simulation. *Energy* **198**, 117296 (2020).

89. Tavares, R., Ramos, A. & Rouboa, A. Microplastics thermal treatment by polyethylene terephthalate-biomass gasification. *Energy Convers. Manag.* **162**, 118–131 (2018).

90. Tavares, R., Ramos, A. & Rouboa, A. A theoretical study on municipal solid waste plasma gasification. *Waste Manag.* **90**, 37–45 (2019).

91. AlNouss, A., McKay, G. & Al-Ansari, T. Enhancing waste to hydrogen production through biomass feedstock blending: A techno-economic-environmental evaluation. *Appl. Energy* **266**, 114885 (2020).

92. Salkuyeh, Y. K., Saville, B. A. & MacLean, H. L. Techno-economic analysis and life cycle assessment of hydrogen production from different biomass gasification processes. *Int. J. Hydrogen Energy* **43**, 9514–9528 (2018).

93. Hasan, A. & Dincer, I. Comparative assessment of various gasification fuels with waste tires for hydrogen production. *Int. J. Hydrogen Energy* **44**, 18818–18826 (2019).

94. Higman, C. & Van der Burgt, M. *Gasification.* (Gulf professional publishing, 2008).

95. Niu, M., Huang, Y., Jin, B. & Wang, X. Simulation of syngas production from municipal solid waste gasification in a bubbling fluidized bed using aspen plus. *Ind. Eng. Chem. Res.* **52**, 14768–14775 (2013).

96. Oyedeji, O. A. Understanding and modeling the formation of syngas contaminants during biomass gasification. (University of Tennessee, Knoxville, 2019).

97. Chutichai, B., Patcharavorachot, Y., Assabumrungrat, S. & Arpornwichanop, A. Parametric analysis of a circulating fluidized bed biomass gasifier for hydrogen production. *Energy* **82**, 406–413 (2015).

98. He, M. et al. Hydrogen-rich gas from catalytic steam gasification of municipal solid waste (MSW): Influence of catalyst and temperature on yield and product composition. *Int. J. Hydrogen Energy* **34**, 195–203 (2009).

99. Ruoppolo, G., Ammendola, P., Chirone, R. & Miccio, F. H2-rich syngas production by fluidized bed gasification of biomass and plastic fuel. *Waste Manag.* **32**, 724–732 (2012).

100. Wilk, V. & Hofbauer, H. Conversion of mixed plastic wastes in a dual fluidized bed steam gasifier. *Fuel* **107**, 787–799 (2013).

101. Porcu, A. et al. Techno-economic analysis of a small-scale biomass-to-energy BFB gasification-based system. *Energies* **12**, 494 (2019).

102. Woolcock, P. J. & Brown, R. C. A review of cleaning technologies for biomass-derived syngas. *Biomass and Bioenergy* **52**, 54–84 (2013).

103. Brown, N. R. Hot gas cleanup of biomass-derived syngas from a pilot-scale, air-blown, fluidized bed gasifier by. (Iowa State University, 2004).

104. Unyaphan, S., Tarnpradab, T., Takahashi, F. & Yoshikawa, K. An investigation of low cost and effective tar removal techniques by venturi scrubber producing syngas microbubbles and absorbent regeneration for biomass gasification. *Energy Procedia* **105**, 406–412 (2017).

105. Tian, F. J., Yu, J., McKenzie, L. J., Hayashi, J. I. & Li, C. Z. Conversion of fuel-N into HCN and NH3 during the pyrolysis and gasification in steam: A comparative study of coal and biomass. *Energy and Fuels* **21**, 517–521 (2007).

106. Dutta, A. et al. *Process Design and Economics for the Conversion of Lignocellulosic Biomass to Hydrocarbon Fuels Thermochemical Research Pathways with In Situ and Ex Situ Upgrading of Fast Pyrolysis Vapors.* https://www.nrel.gov/docs/fy15osti/62455.pdf (2015).

107. Khakharia, P. et al. Acid wash scrubbing as a countermeasure for ammonia emissions from a postcombustion CO2 Capture Plant. *Ind. Eng. Chem. Res.* **53**, 13195–13204 (2014).

108. Nazir, H. et al. Is the H2 economy realizable in the foreseeable future? Part II: H2 storage, transportation, and distribution. *Int. J. Hydrogen Energy* **45**, 20693–20708 (2020).

109. Müller, K., Brooks, K. & Autrey, T. Releasing hydrogen at high pressures from liquid carriers: aspects for the H2 delivery to fueling stations. *Energy and Fuels* **32**, 10008–100015 (2018).

110. Humbird, D. et al. *Process design and economics for biochemical conversion of lignocellulosic biomass to ethanol: dilute-acid pretreatment and enzymatic hydrolysis of corn stover.* https://www.osti.gov/biblio/1013269/ (2011).

111. Davis, R. et al. *Process Design and Economics for the Conversion of Lignocellulosic Biomass to Hydrocarbon Fuels and Coproducts: 2018 Biochemical Design Case Update: Biochemical Deconstruction and Conversion of Biomass to Fuels and Products via Integrated Biorefinery Path.* https://www.nrel.gov/docs/fy19osti/71949.pdf (2018).

112. Wang, X. & Song, C. Carbon capture from flue gas and the atmosphere: a perspective. *Front. Energy Res.* **8**, 560849 (2020).

113. Wang, Y., Zhao, L., Otto, A., Robinius, M. & Stolten, D. A review of post-combustion CO2 capture technologies from coal-fired power plants. *Energy Procedia* **114**, 650–665 (2017).

114. Gaurina-Međimurec, N., Novak-Mavar, K. & Majić, M. Carbon capture and storage (CCS): Technology, projects and monitoring review. *Rud. Geol. Naft. Zb.* **33**, 1–14 (2018).

115. Rao, A. B. & Rubin, E. S. Identifying cost-effective CO2 control levels for amine-based CO2 capture systems. *Ind. Eng. Chem. Res.* **45**, 2421–2429 (2006).

116. US IRS. Cost Segregation ATG - Chapter 6.3 - Depreciation Overview. https://www.irs.gov/businesses/cost-segregation-atg-chapter-6-3-depreciation-overview#2 (2021).

117. Chemical Engineering Magazine. Plant Cost Index. Chemical Engineering Magazine. https://chemengonline.com/ (2015).

118. US BLS. Producer Price Indexes. https://www.bls.gov/ppi/ (2020).

119. US Environmental Protection Agency. AP 42, Fifth Edition compilation of air pollutant emissions factors, Volume 1: Stationary Point and Area Sources. https://www.epa.gov/air-emissions-factors-and-quantification/ap-42-compilation-air-emissions-factors (2009).

120. Wernet, G. et al. The ecoinvent database version 3 (part I): overview and methodology. *Int. J. Life Cycle Assess.* **21**, 1218–1230 (2016).

Acknowledgements

Author contributions

K.L and Y.Y. designed the study. K.L. collected the data and performed the simulation. K.L. analyzed the results. Y.Y. supervised the study. K.L and Y.Y wrote the manuscript.

Competing interests

The authors declare no competing interests.

Additional information

Supplementary information The online version contains supplementary material available at https://doi.org/10.1038/s43247-022-00632-1.

Correspondence and requests for materials should be addressed to Yuan Yao.

Peer review information *Communications Earth & Environment* thanks Valerie Thomas and the other, anonymous, reviewer(s) for their contribution to the peer review of this work. Primary Handling Editors: Alessandro Rubino, Joe Aslin and Clare Davis.

Reprints and permission information is available at http://www.nature.com/reprints

Publisher's note Springer Nature remains neutral with regard to jurisdictional claims in published maps and institutional affiliations.